Chemical Engineering Communications

ISSN: 0098-6445 (Print) 1563-5201 (Online) Journal homepage: http://www.tandfonline.com/loi/gcec20

A CHROMATOGRAPHIC STUDY OF CARBON MONOXIDE ADSORPTION ON A CLINOPTILOLITE-CONTAINING NATURAL ZEOLITIC MATERIAL

G. NARIN , S. YILMAZ & S. ÜLKÜ

To cite this article: G. NARIN , S. YILMAZ & S. ÜLKÜ (2004) A CHROMATOGRAPHIC STUDY OF CARBON MONOXIDE ADSORPTION ON A CLINOPTILOLITE-CONTAINING NATURAL ZEOLITIC MATERIAL, Chemical Engineering Communications, 191:11, 1525-1538, DOI: 10.1080/00986440490472643

To link to this article: http://dx.doi.org/10.1080/00986440490472643

Published online: 11 Aug 2010.

Chem. Eng. Comm., 191: 1525–1538, 2004

ISSN: 0098-6445 print/1563-5201 online
DOI: 10.1080/00986440490472643

Taylor & Francis
Taylor & Francis Group

A CHROMATOGRAPHIC STUDY OF CARBON MONOXIDE ADSORPTION ON A CLINOPTILOLITE-CONTAINING NATURAL ZEOLITIC MATERIAL

G. NARIN
S. YILMAZ
S. ÜLKÜ

Department of Chemical Engineering,
Izmir Institute of Technology,
İzmir, Turkey

In this study, the equilibrium and kinetic parameters for CO adsorption on clinoptilolite-rich natural zeolitic material were determined by the concentration pulse chromatography technique. Experiments were carried out at different column temperatures (60–120°C) and interstitial carrier gas velocities (3.1–16.3 cm/s) using a clinoptilolite-rich natural zeolitic material packed column. The equilibrium and kinetic parameters were determined by matching the moments of the experimentally obtained response curves to the parameters in the mathematical model. The Henry's Law constants were found to decrease from 700 to 49 with increasing temperature. The heat of adsorption at low coverage was found to be 50.73 kJ/molK. The contributions from external film, macropore, and micropore diffusion resistances to mass transfer were determined, and the micropore diffusion resistance was found to be the major contributor. The micropore diffusivity as a function of crystal radius (D_c/r_c^2) was determined and found to change between 5.72×10^{-4} and 1.34×10^{-2} s^{-1} in the temperature range studied.

Keywords: Clinoptilolite; Adsorption equilibrium; Diffusion; Carbon monoxide; Gas chromatography

Received 1 July 2001; in final form 5 December 2002.

Address correspondence to S. Yilmaz, Department of Chemical Engineering, Izmir Institute of Technology, İzmir, Turkey. E-mail: selahattinyilmaz@iyte.edu.tr

INTRODUCTION

Carbon monoxide is mainly emitted from power plants, chemical and metallurgical processes, municipal incinerators, petroleum refineries, cement plants, nitric and sulphuric acid plants, solid waste disposal areas, and agricultural combustion facilities. It contributes to photochemical smog together with high concentrations of particulate matter, SO_2, and NO_2 and plays an important role in ozone depletion. Increasing international environmental concern is forcing industry to develop effective and economically feasible methods to reduce these pollutant emissions to acceptable levels.

Adsorption is widely used in environmental technology for pollutant removal because of its low energy consumption and its suitability for low sorbate concentrations. The principle of adsorption and separation is based on differences in adsorption equilibrium and in intraparticle diffusions of the components. Thus, the design of an effective adsorption and separation process requires the determination of equilibrium and kinetic parameters for the adsorbate-adsorbent pair of interest (Ruthven, 1984; Suzuki, 1990). Adsorption and separation processes generally employ beds of microporous adsorbents such as alumina and silica gel, activated carbons, and synthetic and natural zeolites. Zeolites, which possess uniform pore size distribution (3–10 Å) and thus molecular sieve properties, differ from other types of sorbents (Breck, 1974).

Although the application of synthetic zeolites to gas adsorption and separation has been frequently investigated (Ma and Mancel, 1972; Ruthven, 1976; Haq and Ruthven, 1986a, b), corresponding studies in the case of natural zeolites are rather rare. Adsorption characteristics of H-mordenite, chabazite, and 4A and 5A molecular sieve zeolites for N_2, CO, and CH_4 gases were compared using the chromatographic method over the temperature range of −10 to 60°C in the carrier gas flow rate range of 13–33 mL/min (Tezel and Apolonatos, 1993). The strong adsorption of CO on H-mordenite and 5A zeolite was attributed to their large surface area and pore size. Micropore diffusion of CO was not found as a dominant mass transfer mechanism in any of the adsorbents.

In another study, N_2, CO, CO_2, and NO adsorption characteristics of a Turkish clinoptilolite, 5A, 4A, H-mordenite, and activated carbon were tested chromatographically (Triebe and Tezel, 1995a). The clinoptilolite showed the highest Henry's Law constants for all gases in the temperature range of 75–150°C. The stronger adsorption of CO on clinoptilolite was explained by formation of a complex between CO and divalent cations in the clinoptilolite structure. Micropore diffusion was found to be the dominant diffusion mechanism of CO in clinoptilolite for the carrier gas flow rate between 7 and 15 mL/min. Triebe et al. (1993) also investigated the utilization of a natural clinoptilolite from Turkey in air

purification and separation, in the temperature range from −30 to 200°C using a gas chromatographic technique. Higher heat of adsorption values for CO, N_2, and NO on clinoptilolite were obtained than those on 4A and 5A zeolites and H-mordenite. Furthermore, clinoptilolite exhibited the highest separation factors for NO/N_2 and CO/N_2 systems.

The adsorption capacity of a Turkish clinoptilolite for CO was determined by concentration pulse chromatography and found to be 20 mL(STP)/g up to a pressure of 101.3 kPa at 30°C (Triebe and Tezel, 1995b). The binary adsorption studies showed that CO was adsorbed 5 to 10 times faster than N_2. Sirkecioğlu et al. (1995) similarly obtained 31 mL(STP)/g CO adsorption capacity for clinoptilolite at 20°C by the volumetric method. There also have been some studies on the use of clinoptilolite-rich zeolitic materials in air drying applications, investigating mineralogical, chemical, and thermal properties, and effects of cation content on gas adsorption properties (Ülkü et al., 1992; Özkan and Ülkü, 1998; Sirkecioğlu et al., 1991; Esenli and Kumbasar, 1994; Erdem-Şenatalar et al., 1993).

The data on the adsorption properties of clinoptilolite-rich zeolitic material for different gases showed that it could be a good adsorbent for gas adsorption and separation applications. However, the determination of suitability and efficiency of clinoptilolite for these applications requires further studies. Thus, in this study, special interest has been devoted to determination of adsorption and diffusion properties of clinoptilolite-rich tuff, which is available in large quantities in middle western Anatolia, Turkey.

THEORY

Estimation of equilibrium and kinetic parameters for the specific adsorbate/adsorbent pair by chromatographic method requires matching of experimental peak data to suitable mathematical model parameters. The first and second moments of the experimentally obtained chromatographic response peaks are directly calculated from numerical peak data by integrating the following expressions:

$$\bar{\mu} = \frac{\int_0^\infty tc(t)dt}{\int_0^\infty c(t)dt} \tag{1}$$

$$\bar{\sigma}^2 = \frac{\int_0^\infty (t-\bar{\mu})^2 c(t)dt}{\int_0^\infty c(t)dt} \tag{2}$$

Since the moments for a packed column also contain contributions due to non-column effects (gas flow between the injector and the column inlet,

between the outlet of the column and the detector), the net moments are calculated by subtracting the moments for an empty column from those for a packed column (Hufton, 1992).

The dynamic model developed by Haynes and Sarma (1973) offers the most suitable model to describe diffusion and adsorption in a column packed with biporous adsorbent. This model assumes low sorbate concentrations, isothermal operation, axially dispersed plug flow regime in the column, instantaneous equilibrium between the sorbate and adsorbent, and negligible pressure drop across the column. Then, the net first moment of a pulse is approximately proportional to both the equilibrium constant (K) and the residence time of a carrier gas (L/v) as

$$\mu = \frac{L}{v}\left[1 + \left(\frac{1-\varepsilon}{\varepsilon}\right)K\right] \tag{3}$$

Temperature dependence of the Henry's Law constant is given by the van't Hoff equation as

$$K = K_o \exp(-\Delta U_o/RT) \tag{4}$$

The heat of adsorption at low coverage (ΔH_o) is determined using the intercept and slope of the van't Hoff plot as

$$-\Delta H_o = -\Delta U_o + RT \tag{5}$$

where T is taken as the mean of the experimental temperature range.

For gaseous systems, the general form of the second moment for a biporous adsorbent including the contributions from axial dispersion and mass transfer resistances is expressed as

$$\frac{\sigma^2 L}{2\mu^2 v} = \frac{D_L}{v^2} + \frac{\varepsilon}{\varepsilon - 1}\left(\frac{R_p}{3k} + \frac{R_p^2}{15\varepsilon_p D_p} + \frac{r_c^2}{15 D_c K}\right) \tag{6}$$

The contributions from axial dispersion and mass transfer resistance can be distinguished by performing measurements over a range of fluid velocities. At low Re, axial dispersion occurs primarily by molecular diffusion and thus D_L is independent of the velocity. The external film resistance is correlated in terms of Sh using an empirical expression suggested by Ranz and Marshall for packed columns as (Ruthven, 1984)

$$Sh = \frac{2R_p k}{D_m} = 2 + 0.6 Sc^{0.33} \mathrm{Re}^{0.5} \tag{7}$$

The macropore diffusivity (D_p), assuming that both molecular and Knudsen diffusion mechanisms are significant, is calculated by

$$\frac{1}{D_p} = \tau\left(\frac{1}{D_m} + \frac{1}{D_K}\right) \tag{8}$$

where τ is the tortuosity factor characterizing the shape and orientation of the pores; experimental values of τ are reported in the range of 1.7 to 6 (Ruthven, 1984).

The contribution of micropore diffusion resistance can be determined subtracting other mass transfer resistances from the total mass transfer resistance. The temperature dependence of the micropore diffusion coefficient may be expressed by an Arhenius type equation (Kärger and Ruthven, 1992):

$$D_c = D_o \exp(-E_a/RT) \tag{9}$$

EXPERIMENTAL

Material and Characterization

Clinoptilolite-rich natural zeolitic material from Gördes, middle western Anatolia, was used as adsorbent in this study. The particle size distribution of the washed sample was determined via Malvern Mastersizer S Ver.2.14. The chemical composition of the washed clinoptilolite-rich zeolitic material was investigated by Varian Model Liberty II ICP-AES (inductively coupled plasma–atomic emission spectroscopy).

X-ray diffraction (XRD) analysis was used for identification of the zeolitic material and for comparison of crystallinity of the samples after various thermal treatments using Philips X'Pert diffractometer at the 1.541 Å wavelength of CuK_α radiation, between angles of 5 and 40°, 2θ, at a rate of 0.05°/s. The zeolite samples were ground to less than 75 μm for XRD analysis.

Thermogravimetric analyses (TGA) were performed by Shimadzu TGA-51 up to the maximum temperature of 800°C under different N_2 flow rates (5, 10, and 20 mL/min) and different heating rates (2, 5, and 10°C/min). Differential thermal analyses were carried out by a Shimadzu DTA-50 up to the maximum temperature of 1000°C at 5°C/min heating rate.

Textural properties (pore volume, surface area) and adsorption isotherms for both unwashed and washed samples were determined volumetrically by a Micromeritics ASAP 2010 by Argon at 87.40 K.

Apparatus and Method

A Shimadzu GC-17A Ver. 3 gas chromatograph (GC) equipped with thermal conductivity detector (TCD) was used for all chromatographic

experiments. Ultrahigh purity He (99.999%) was used as carrier gas. A digital mass flow controller was used for adjustment of the carrier gas flow rate. Oxygen and molecular sieve traps were employed to remove impurities in the carrier gas. A 0.25 mL CO injection pulse was introduced to the column by means of a sampling valve.

The washed and sieved clinoptilolite particles were packed into the stainless steel column. The adsorption column characteristics are given in Table I. The column porosity was calculated from the apparent density of the natural zeolitic material, determined as 1.24 g/cm^3 by weighing a cubic specimen of the zeolitic material of known volume after drying at 400°C for 6 hours; TGA analysis showed that there was no further weight loss for longer duration. The pressure drop across the packed column was calculated in the range of 0.11–0.67 kPa using Ergun's correlation and found to be negligible (Ergun, 1952). The regeneration was carried out within the GC oven first at 100°C for 2 hours and then at 350°C for 24 hours under 50 mL/min helium purge to remove impurities and moisture. The GC oven temperature increased in steps of 10°C/min up to 350°C, then was allowed to cool to the analysis temperatures. The carrier gas flow was maintained in the system for purging between the experimental runs.

Gas Chromatographic Experiments

Prior to the chromatographic experiments, the linearity of the detector response with the inlet CO concentration was tested by injecting 0.25 mL gas pulses of different CO concentrations into the empty column. Adsorption equilibrium and kinetic experiments were performed by gas chromatography at the column temperatures of 60, 80, 100, and 120°C and carrier gas flow rates in the range of 9 to 40 mL/min, corresponding to the interstitial carrier gas velocities in the 3.1–16.3 cm/s range. The CO pulse was injected after the column was brought to equilibrium. Before the packed column experiments, empty column measurements were performed in order to determine the dead moments.

Table I. Packed column characteristics

Mass of packing	1.389 g
Particle size range	500–850 μm
Mean particle diameter	602.5 μm
Column internal diameter	0.46 cm
Column length	10 cm
Bed porosity, ε	0.33
Particle porosity, ε_p	0.34[a]
Bed density	0.84 g/cm^3

[a]Breck, 1974

RESULTS AND DISCUSSION

Characterization

The particle size distribution exhibited a narrow size range (500−850 μm) around the mean diameter of 602.5 μm. The chemical composition of the washed clinoptilolite-rich zeolitic material is given in Table II. Si/Al ratio of the tuff was found to be 5.84.

The results of the X-ray diffraction analyses are given in Figure 1 showing that clinoptilolite was the main mineral phase in the natural zeolite material examined. The characteristic peaks of clinoptilolite were observed at $2\theta = 9.93°$, 22.48° and 30.18°. The adsorbent contains about 80% clinoptilolite, 5−8% opal-CT, 4−5% feldspar, 3% quartz, and 1−2% biotite. The XRD analysis results showed good agreement with the previously reported composition data for the natural zeolitic material from the same region (Esenli, 1992; Esenli and Kumbasar, 1998). The crystallinities of the samples treated at 400°C for 6 hours and regenerated for gas chromatographic experiments (at 350°C for 24 hours under helium purge) were also checked by XRD. There were slight changes in the peak intensities, which could be attributed to cation migration and elimination of the water molecules from the channels of the framework due to heating (Arcoya et al., 1996).

Thermogravimetric analysis showed that the average percent weight loss up to 800°C was 10.54 for unwashed and 10.88 for washed samples. The destruction temperature of the clinoptilolite was determined as about

Table II. Chemical composition of the used Zeolitic material as % weight

Material	% weight
Al_2O_3	12.354
CaO	4.906
Fe_2O_3	1.561
K_2O	3.276
MgO	1.265
Na_2O	1.176
B_2O_3	0.144
BaO	0.066
CuO	0.092
NiO	0.177
ZnO	0.303
SiO_2	72.100
Others (Ag_2O, Co_3O_4, Cr_2O, MnO, PbO)	0.059

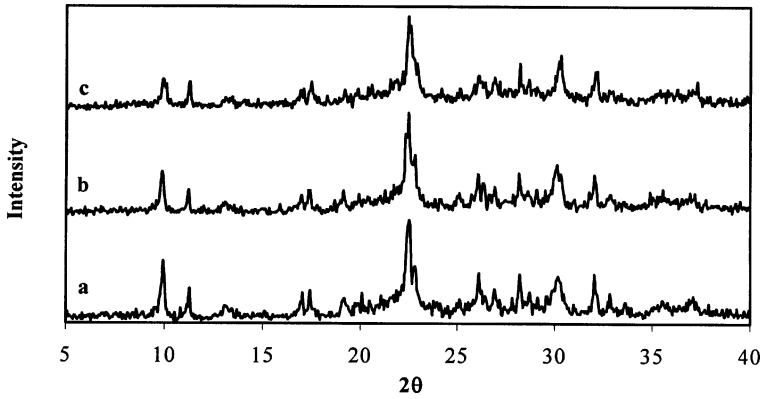

Figure 1. X-ray diffraction patterns of the natural zeolitic materials; (a) washed and dried overnight at 105°C, (b) treated at 400°C for 6 h, (c) regenerated for gas chromatographic experiments.

840°C. This high destruction temperature was attributed to its high Si/Al ratio (5.84).

Volumetric adsorption analyses exhibited typical Type IV isotherms for both unwashed and washed samples. The higher adsorption capacity of the washed sample can most probably explained by the removal of soluble phases from the sample and eventual zeolite enrichment of the sample. The specific surface area of the washed sample was determined as 33.11 m^2/g by the BET model. Cumulative surface area, pore volume, and average mesopore diameter were obtained by the BJH method as 33.55 m^2/g, 0.039 cm^3/g, and 46.28 Å, respectively. Maximum pore volume and median micropore diameter were calculated as 0.0103 cm^3/g and 8.49 Å, respectively by the Horvath-Kawazoe model. The Dubinin-Astakhov model was applied to determine the micropore surface area and found to be 50.89 m^2/g. These results are given only for comparison purposes since only pore sizes of the clinoptilolite that are large enough to allow Ar molecules to enter the pores were determined.

Gas Chromatographic Experiments

Symmetric response peaks were obtained for the empty column, while the peaks for the packed column were tailed, indicating the existence of significant internal diffusion (micropore and mesopore) resistances (Kärger and Ruthven, 1992).

The net first and second moments were calculated from the chromatographic peak data using Equations (1) and (2). Percentages of moments contributed by empty column to the packed column moments for each temperature are given in Table III. Linear plots of net first

Table III. Contribution from empty column moments to the packed column moments

T (°C)	Empty column first moment contribution (%)	Empty column second moment contribution (%)
60	5.27–8.66	0.07–0.50
80	10.01–19.79	0.50–3.69
100	22.64–33.22	2.01–13.82
120	42.73–72.99	24.23–75.09

moments versus reciprocal interstitial carrier gas velocity confirmed that equilibrium was reached in the column for the temperature range covered in the study.

The dimensionless Henry's Law constants were derived from Equation (3) and found to decrease from 699.8 to 49.1 with increasing temperature. The K values were plotted against reciprocal temperature as shown in Figure 2. K_o and $-\Delta U_o$ were then derived from the intercepts and slopes of these plots, respectively, as given by Equation (4). Using Equation (5), $-\Delta H_o$ was calculated as 50.73 kJ/molK. The comparison of K_o, $-\Delta U_o$, and $-\Delta H_o$ values with the values from other studies is summarized in Table IV. The higher $-\Delta H_o$ value obtained in the present study might be explained by the strong interaction of CO with the clinoptilolite-rich natural zeolitic material due to the different natures of adsorbate-adsorbent interactions depending on the structure and divalent cation content (Ca^{2+} and Mg^{2+}) of the zeolitic material (Arcoya et al., 1996).

The mass transfer coefficients were determined by matching the experimentally determined second moments to the model parameters in

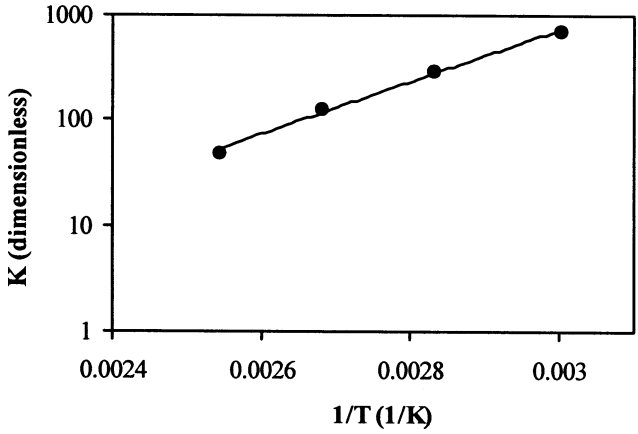

Figure 2. Dependence of Henry's Law constants on column temperature (van't Hoff plots).

Table IV. Parameters K_o, $-\Delta U_o$, and $-\Delta H_o$ for CO adsorption on different adsorbents

Adsorbent	Reference	T (°C)	Average K_o (dimensionless)	$-\Delta U_o$ (kJ/mol)	$-\Delta H_o$ (kJ/mol)
Clinoptilolite	Present study	60–120	2.43×10^{-5}	47.71	50.73
Clinoptilolite		50–200	7.3×10^{-5}	45.2	48.5
4A		–30–90	2.2×10^{-3}	25.1	27.6
5A	Triebe and Tezel (1995a)	–10–90	6.2×10^{-3}	30.1	32.6
H-mordenite		30–60	5.0×10^{-3}	20.9	23.4
Activated carbon		30–150	4.4×10^{-3}	14.6	17.6
5A		30–150	–	–	28.4
H-mordenite	Tezel and Apolonatos (1993)	–10–90	–	–	25.1

Equation (6). The contributions from axial dispersion and other mass transfer resistances were determined by plotting total dispersion ($\sigma^2 L/2\mu^2 v$) versus $1/v^2$ for different temperatures, as shown in Figure 3.

The total dispersion increased gradually with velocity. The linearity of these plots confirmed that D_L is independent of velocity over the velocity range covered in the experiments. The D_L values determined

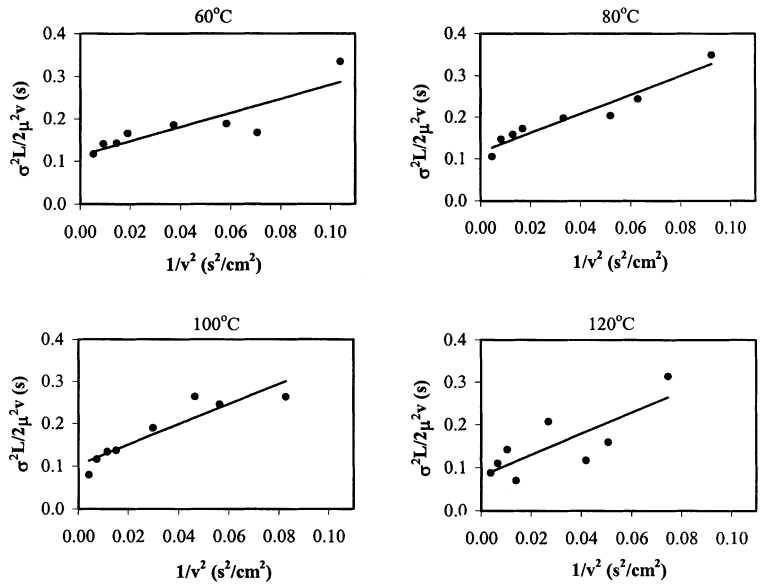

Figure 3. Dependence of total dispersion on carrier gas velocity at different column temperatures.

from the slopes can be expressed as $D_L \cong 2.2\, D_m$. The total mass transfer resistance was determined from the intercepts. The contribution of each resistance is given in Table V. The contribution from external mass transfer resistance ($R_p/3D_m$) was estimated using Equation (7) and found to be negligible. The macropore diffusivity was calculated from Equation (8) using the typical τ value of 3, and the corresponding diffusion resistance ($R_p^2/15\epsilon_p D_p$) was calculated. The micropore diffusion resistance ($r_c^2/15KD_c$) was determined by subtracting the sum of external film and macropore diffusion resistances from the total mass transfer resistance according to Equation (6).

The variation of the intercepts of Figure 3 with column temperature is plotted in Figure 4. The intercepts decreased significantly with increasing temperature, suggesting that the micropore diffusion resistance was the dominant resistance under the experimental conditions investigated, since the resistances contributing to the CO diffusion other

Table V. Contributions to the total mass transfer resistance

T (°C)	$R_p^2/15\varepsilon_p D_p$ (s)	$R_p/3D_m$ (s)	Total Mass Transfer Resistance (s)	$r_c^2/15KD_c$ (s)
60	0.0695	3.61×10^{-4}	0.2364	0.1665
80	0.0677	3.26×10^{-4}	0.2406	0.1726
100	0.0657	2.98×10^{-4}	0.2136	0.1476
120	0.0640	2.74×10^{-4}	0.1659	0.1016

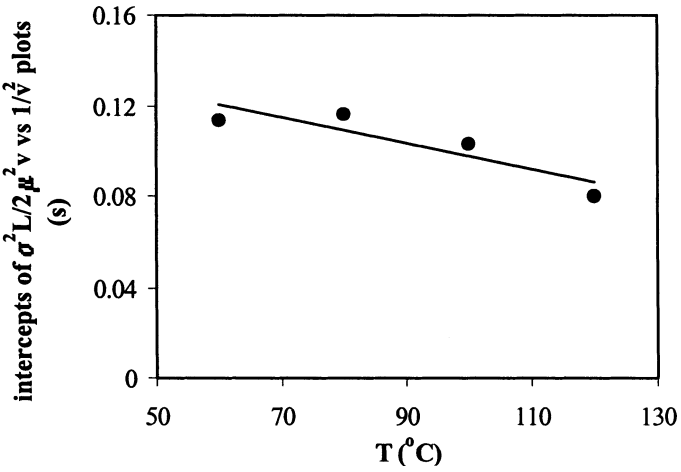

Figure 4. Dependence of intercepts of the total dispersion versus $1/v^2$ plots on column temperature.

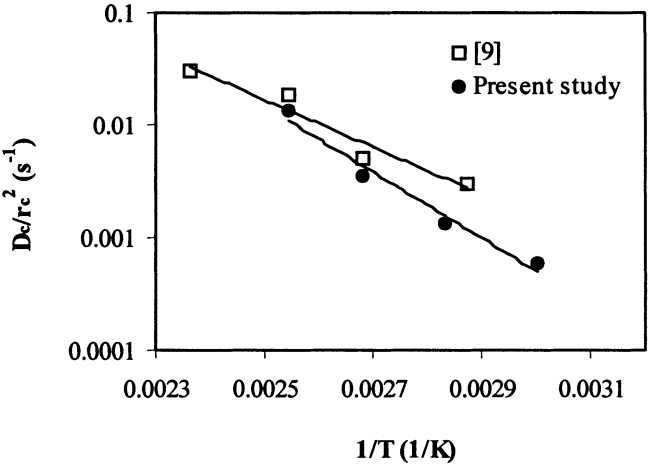

Figure 5. Temperature dependence of D_c/r_c^2.

Table VI. Parameters D_o/r_c^2 and E_a

T Range (°C)	D_o/r_c^2 (s^{-1})	E_a (kcal/mol)	Reference
60–120	3.38×10^5	13.5	Present study
75–150	4.60×10^3	10.0	Triebe and Tezel (1995a)

than micropore diffusion are weak functions of temperature (Triebe and Tezel, 1995a; Kärger and Ruthven, 1992).

The micropore diffusivity parameters (D_c/r_c^2) were calculated from micropore resistances. The variation of D_c/r_c^2 with temperature is presented in Figure 5, together with the data from a previous study (Triebe and Tezel, 1995a). The D_c/r_c^2 increased with increasing temperature as expected. The parameters D_o/r_c^2 and E_a were derived from the intercept and slope using Equation (9), respectively, and compared with the data reported in the literature in Table VI. The higher E_a values determined in the present study could be explained by higher barrier to adsorption due to the divalent cation content of the zeolitic material with which CO molecules interact strongly (Triebe and Tezel, 1995a).

CONCLUSIONS

The Henry's Law constants decreased with increasing temperature. The heat of adsorption at low coverage was found to be 50.73 kJ/mol. The difference between the calculated heats of adsorption and those in

the literature was attributed to the pore size, cation content, and accessibility of cations in the clinoptilolite framework. The total mass transfer resistance, including external mass transfer, micropore, and macropore diffusion resistances, was determined experimentally and found to be in the range of 0.166–0.241 s. The micropore diffusion resistance was determined as the major contributor to the diffusion of CO in clinoptilolite-rich natural zeolitic material controlling the overall mass transfer. The diffusional activation energy for diffusion was also determined.

ACKNOWLEDGMENT

Financial support of the Turkish Republic State Planning Organization is gratefully acknowledged.

NOMENCLATURE

$c(t)$	adsorbate concentration in the bulk phase measured by detector
D_c	micropore diffusion coefficient
D_K	Knudsen diffusion coefficient
D_L	axial dispersion coefficient
D_m	molecular diffusion coefficient
D_o	temperature-independent diffusion constant
D_p	macropore diffusion coefficient
E_a	diffusional activation energy
ΔH_o	heat of adsorption at low coverage
k	external film mass transfer coefficient
K	dimensionless Henry's Law constant
K_o	pre-exponential factor
L	column length
R	universal gas constant
r_c	radius of zeolite crystal
R_p	radius of zeolite particle
Re	Reynolds number
Sc	Schmidt number
Sh	Sherwood number
T	temperature
ΔU_o	internal energy change of adsorption
v	interstitial carrier gas velocity

Greek letters

ε	bed porosity
ε_p	particle porosity
μ	net first moment of response peak
$\bar{\mu}$	first moment of experimentally obtained response peak
σ^2	net second moment of response peak
$\bar{\sigma}^2$	second moment of experimentally obtained response peak
τ	tortuosity factor

REFERENCES

Arcoya, A., Gonzalez, J. A., Llarbe, G., Seone, X. L., and Travesio, N. (1996). *Microporous Mater.*, **7**, 1–13.

Breck, D. W. (1974). *Zeolite Molecular Sieves*, Wiley-Interscience, New York.

Erdem-Şenatalar, A., Sirkecioğlu, A., Güray, I., Esenli, F., and Kumbasar, I. (1993). *Proceedings from the 9th International Zeolite Conference, Montreal*, eds. R. von Ballmoos, J. B. Higgins, and M. M. J. Treacy, Vol. 2, 223–231, Butterworth-Heinemann, Boston.

Ergun, S. (1952). *Chem. Eng. Prog*, **48**, 89.

Esenli, F. (1992). Gördes ve Çevresindeki Neojen Serilerin ve Zeolitleşmenin Jeolojik, Mineralojik ve Jeokimyasal İncelenmesi, Ph.D diss., 209, Istanbul Technical University.

Esenli, F. and Kumbasar, I. (1994). In *Zeolite and Related Microporous Materials: State of the Art 1994*, eds. J. Weitkamp, H. G. Karge, H. Pfeifer, and W. Hölderich 645–651; Elsevier Science, New York.

Esenli, F. and Kumbasar, I. (1998). *Clays Clay Miner.*, **46**, 679–686.

Haq, N. and Ruthven, D. M. (1986a). *J. Coll. Interface Sci.*, **112**, 154–163.

Haq, N. and Ruthven, D. M. (1986b). *J. Coll. Interface Sci.*, **112**, 164–169.

Haynes, Jr., H. W. and Sarma, P. N. (1973). *AIChE J.*, **19**, 1043–1046.

Hufton, J. R. (1992). Diffusion and Equilibrium of Alkanes on Silicalite Determined by Perturbation Chromatography, Ph.D diss., The Pennsylvania State University.

Kärger, J. and Ruthven, D. M. (1992). *Diffusion in Zeolites and Other Microporous Solids*, John Wiley, New York.

Ma, Y. H. and Mancel, C. (1972). *AIChE J.*, **18**(6), 1148–1153.

Özkan, F. and Ülkü, S. (1998). *Plastik ve Ambalaj Teknolojisi, Sayi*, **25**, 102–110.

Ruthven, D. M. (1976). *AIChE J.*, **22**, 753–759.

Ruthven, D. M. (1984). *Principles of Adsorption and Adsorption Processes*, John Wiley, New York.

Sirkecioğlu, A., Esenli, K., Kumbasar, I., Eren, R. H., and Erdem-Şenatalar, A. (1991). In *Proceedings of the International Earth Science Congress on Aegean Regions (IESCA), İzmir*, eds. M. Y. Savascin and A. H. Eronat, Vol. 1, 291–301.

Sirkecioğlu, A., Altav, Y., and Erdem-Şenatalar, A. (1995). *Sep. Sci. Technol.*, **30**(13), 2747–2762.

Suzuki, M. (1990). *Adsorption Engineering*, Elsevier, Amsterdam.

Tezel, F. H. and Apolonatos, G. (1993). *Gas Sep. Purif.*, **7**, 11–17.

Triebe, R. W. and Tezel, F. H. (1995a). *Gas Sep. Purif.*, **9**(4), 223–230.

Triebe, R. W. and Tezel, F. H. (1995b). *Can. J. Chem. Eng.*, **73**, 717–724.

Triebe, R. W., Tezel, F. H., Erdem-Şenatalar, A. and Sirkecioğlu, A. (1993). In *Zeolite Science 1994: Recent Progress and Discussions*, 219–220; Elsevier, New York.

Ülkü, S., Balköse, D., Baltacioğlu, H., Özkan, K., and Yildirim, A. (1992). *Dry. Technol.*, **10**(2), 475–490.